Morphology of Voids in Molecular Systems. A Voronoi−Delaunay Analysis of a Simulated DMPC Membrane

Marina G. Alinchenko and Alexey V. Anikeenko

Institute of Chemical Kinetics and Combustion, Siberian Branch of the RAS, Group of Supramolecular Structures, Institutskaya 3, R-630090 Novosibirsk, Russia, and Novosibirsk State University, Novosibirsk, Russia

Nikolai N. Medvedev and Vladimir P. Voloshin

Institute of Chemical Kinetics and Combustion, Siberian Branch of the RAS, Group of Supramolecular Structures, Institutskaya 3, R-630090 Novosibirsk, Russia

Mihaly Mezei

Department of Physiology and Biophysics, Mount Sinai School of Medicine, New York University, 1 Gustave L. Levy Place, New York, New York 10029

Pál Jedlovszky*

Department of Colloid Chemistry, Eötvös Loránd University, Pázmány Péter stny. 1/a, H-1117 Budapest, Hungary

Received: May 26, 2004; In Final Form: August 31, 2004

A generalized version of the Voronoi−Delaunay method is used to study relatively large intermolecular voids in a model of the hydrated DMPC bilayer, obtained from all-atom Monte Carlo simulation. Application of the original version of the method for molecular systems has been hampered by the fact that these systems geometrically represent ensembles of partially overlapping spheres of different radii. The generalized version of the method is based on using the additively weighed Voronoi diagram, representing the locus of spatial points being equally far from the surface rather than the center of the corresponding pair of atoms. This version of the Voronoi−Delaunay method can be readily used to reveal and analyze voids accessible for probes of different radii even in rather complex molecular systems. When the properties of the voids present in the simulated DMPC membrane are investigated, their shape, size, and orientation have been analyzed in detail in the different regions of the membrane located at different depths along the membrane normal axis. The characteristics of the voids are found to be different in different regions of the bilayer, namely (i) at the middle of the membrane, in the region of the hydrophobic lipid tails, (ii) in the region of the hydrophilic zwitterionic headgroups, and (iii) in the region of the bulklike water adjacent to the bilayer. The largest and oblong voids are found in the middle of the membrane, with a preferred orientation that is parallel to the bilayer normal axis. A clear correlation between the orientation of the voids and the orientation of the lipid chains is observed. In the bulk water region the fraction of the empty space is even higher than at the middle of the membrane; however, here the voids are distributed more uniformly. Finally, in the high-density region of the hydrophilic headgroups the voids are found, on average, smaller than in the other parts of the system.

Introduction

Traditional objects of the structural application of the Voronoi−Delaunay method in the field of physics of condensed matter are the models of systems that are geometrically represented as ensembles of balls of equal radii (e.g., various condensed phases of atomic systems). The applicability of the initial mathematical premises of the method[1,2] is also limited to this case. The method has indeed been used to analyze various properties of systems of this type at the molecular level, such as the local order in noncrystalline packings,[3−11] extended (i.e., intermediate range) structural correlations,[12−14] percolation and properties of the interatomic voids,[15−17] etc. The Voronoi−Delaunay method is still widely applied in its classical form for analyzing different structural aspects of various condensed systems.[18−22]

The application of the method to molecular systems (e.g., molecular liquids, solutions, polymers, biological molecules) might require some modifications of its original version, because these systems often consist of atoms of different sizes. Furthermore, atoms connected by a chemical bond in these systems usually approach each other considerably closer than the sum of their van der Waals radii. Therefore, molecular systems can geometrically be regarded as ensembles of partially overlapping balls of different radii. In analyzing the properties of the empty interatomic space in these systems, we also have to take the above factors into account.

One of the important problems of the application of the method for molecular systems is the determination of the region

* Corresponding author. E-mail: pali@para.chem.elte.hu.

10.1021/jp040386q CCC: $27.50
Published on Web 11/11/2004

of space that can be assigned to a given atom. The Voronoi polyhedron can only be used for this purpose in systems of atoms of equal size, because it neglects atomic radii. Thus, in systems containing atoms of noticeably different sizes, the surface of the Voronoi polyhedron of a large atom can be partly or even fully inside the van der Waals sphere representing the atom, and hence even a part of this van der Waals sphere can be assigned to other atoms. To avoid this problem, the original Voronoi polyhedron has been proposed to be substituted by other constructions that can take atomic sizes also into account. As the simplest way of overcoming this problem, it has been proposed to divide the space between atomic pairs by the planes passing between the atomic surfaces.[23] In this case, the faces of the polyhedron constructed do not intersect the surface of its central atom. However, this idea did not become widely used, because the polyhedra constructed in this way do not provide a correct tessellation of the space (i.e., they can overlap each other as well as can have gaps between them). As a further improvement, the use of the radical tessellation (called also the power[24] or Laguerre tessellation[25] in mathematics) has been proposed.[26,27] This tessellation can be used to correctly divide space among the atoms according to their size. However, despite its interesting mathematical properties,[28] the physical meaning of this tessellation is not obvious. Therefore, the use of the Voronoi S-tessellation[29,30] seems to be more appropriate for this purpose. In constructing this tessellation, the distance of a spatial point from an atom is defined simply as the shortest distance from its surface. For spherical particles, the Voronoi S-tessellation coincides with the known additively weighed Voronoi diagram;[31] however, it can also be defined for bodies of other shapes.[31,32] Some peculiarities[33,34] and mathematical properties[31,35,36] of the Voronoi S-tessellation are discussed in several previous works.

It should be noted, however, that the determination of the Voronoi S-tessellation is far from being obvious. Thus, several attempts have been made to find appropriate algorithms for this problem. Some authors have only considered the problem in two dimensions,[37−39] which, however, does not display some important peculiarities of the 3-dimensional case. The 3D case is discussed in detail by Will[40] and by Richard et al.[41] However, these studies are restricted to the determination of the Voronoi S-regions. Goede et al. have used this method to describe the shape of the surface of complex molecules.[42] In some previous papers we have presented another algorithm and used it for the calculation of the Voronoi S-network.[29,30] However, this algorithm proved to be inefficient for larger models. A specific algorithm for a numerical determination of the S-network in systems consisting of straight lines and spherocylinders has also been described.[32] Recently, we have developed a novel algorithm for constructing the 3D Voronoi S-network in large models.[43]

Another important problem related to the Voronoi analysis of molecular systems is the investigation of the properties of the interatomic voids. The analysis of the interatomic cavities, voids, and pockets differs somewhat from the determination of the volumes assigned to given atoms. This analysis can conveniently be done by using the Delaunay simplexes determined by four mutually neighboring atoms. Such quadruplets of atoms are the simplest elements of the structure in the three-dimensional space, each of them determining an elementary cavity. Any complex void can be composed by such simplex cavities. This property of the Delaunay simplexes has successfully been used to solve various problems in the analysis of interatomic voids in various systems,[14,17,20] including biological ones.[44]

Hydrated phospholipid membranes are rather complex, anisotropic and highly inhomogeneous molecular systems, in which the analysis of the properties of voids cannot be reliably done by the original version of the Voronoi−Delaunay method. The investigation of the properties of the voids in hydrated phospatidylcholine membranes is, however, of particular importance, because these molecules, such as dimyristoylphosphatidylcholine (DMPC) and dipalmitoylphosphatidylcholine (DPPC), are the main components of the membranes of the eukaryotic cells. Although the transport of molecules across biological membranes is usually assisted by various channel-forming proteins, several small, uncharged molecules (e.g., O_2, CO, CO_2, NO) can permeate through the membrane simply by diffusion. Computer simulation investigation of this diffusion process is, however, seriously hindered by the extreme computational effort required by such calculations. To our knowledge, the diffusion profiles of molecules across a hydrated membrane bilayer have only been determined once by computer simulation methods, in the pioneering works of Marrink and Berendsen.[45,46] Indirect information on the permeability of the membrane for various penetrants can be obtained from computer simulation by calculating the free energy profile of the penetrants, i.e., the thermodynamic driving force of their diffusion.[47,48] Furthermore, the properties (e.g., size, shape, and orientation) of the intermolecular voids in the membrane are also obviously related to the membrane permeability, as the possible presence of preformed channels can largely facilitate the diffusion of the molecules of appropriate size. The properties of the voids in a lipid bilayer have, to our knowledge, only been analyzed once, in the fully hydrated DPPC bilayer by Marrink, Sok, and Berendsen using an approximate method (i.e., search along a grid) for locating the voids in the system.[49]

Geometric Concepts of the Voronoi−Delaunay Method

System of Discrete Points or Atoms of the Same Size. In this section we recall the main notions of the original version of the Voronoi−Delaunay method, in which the object of the study is a three-dimensional system of discrete points (centers of atoms), or atoms of equal radii.[1,2] The first construction of the method is the Voronoi polyhedron, i.e., the region of space where all points are closer to the center of a given atom than to the center of any other atom. The Voronoi polyhedra constructed for all atoms of the system form a mosaic, called the Voronoi tessellation, which covers the space without overlaps or gaps. An important property of the Voronoi tessellation is that it defines quadruplets of mutually neighboring atoms, whose particular feature is that the sphere circumscribed around them does not contain any atomic centers. Moreover, the sphere inscribed among the atoms of such quadruplets is empty, i.e., does not overlap with any atoms of the system. Such a quadruplet of atoms determines a tetrahedron, called the Delaunay simplex. Similarly to the Voronoi polyhedra, the Delaunay simplexes constructed for the entire system also form a mosaic covering the space without overlapping and gaps. This mosaic is called the Delaunay tessellation. Thus, the Delaunay simplexes can be regarded as the "bricks" composing the empty interatomic space in an atomic system.

The set of all vertexes and edges of the Voronoi polyhedra forms a singly connected network, called the Voronoi network. The Voronoi network is a geometric construction that can be conveniently used in analyzing spatial structural correlations of the interatomic voids. Each vertex (site) of the Voronoi network corresponds to one of the Delaunay simplexes, being

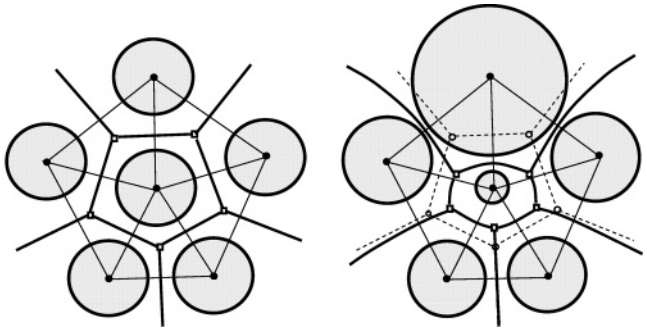

Figure 1. Two-dimensional illustration of the Voronoi regions in a system of balls of the same size (left) and in that of balls of different sizes (right). The edges of the Voronoi regions (i.e., Voronoi polyhedra and Voronoi S-regions in the systems shown on the left and right panel, respectively) are shown by thick lines, and those of the Delaunay simplexes are indicated by thin lines. In the right panel dashed lines depict the edges of the conventional Voronoi polyhedra of the system (same as shown in the left panel).

the center of its circumscribed sphere. Each edge (bond) of the Voronoi network represents a fairway passing through the narrow bottleneck between three atoms from one site to the neighboring one. The basic constructions of the original Voronoi−Delaunay method are illustrated in the left panel of Figure 1 for a system of equal spheres.

System of Atoms of Different Sizes. Consider now the generalization of the Voronoi−Delaunay method that makes it suitable for the analysis of the empty interatomic space in systems consisted of atoms of different sizes.[29,33,34] The basic construction of the generalized method is the Voronoi S-region, i.e., the region of space where all points are closer to the *surface* of a given atom than to that of the other atoms of the system. For atoms of the same size, this region obviously coincides with the Voronoi polyhedron. In the case of atoms of different sizes, however, the faces of the Voronoi S-region are pieces of second-order surfaces rather than planes. Although the metrics and topology of the Voronoi S-region can also characterize the local environment of its central atom,[41] its most important property is to determine the region of space that can be naturally assigned to a given atom. The Voronoi S-regions constructed for all atoms of the system form a mosaic that covers the space without overlapping and gaps. This mosaic is called the Voronoi S-tessellation.

Similarly to the original Voronoi tessellation, the Voronoi S-tessellation can also define quadruplets of mutually neighboring atoms, the sphere inscribed among which is empty. Thus, each quadruplet determines a Delaunay S-simplex and represents an elementary cavity between the atoms. The Delaunay S-simplexes usually coincide with the classical Delaunay simplexes defined for the atomic centers; however, depending on the atomic radii, they can also differ from them.[34] Further, similarly to the classical case, the Voronoi S-network can be defined as the set of the vertexes and edges of all the Voronoi S-regions of the system. Each vertex (site) of the Voronoi S-network is the center of an interstitial sphere, corresponding to one of the Delaunay S-simplexes, whereas each edge (bond) of the network is a fairway passing through the bottleneck between three atoms from one network site to the neighboring one. The Delaunay S-simplexes corresponding to neighboring S-network sites have one face (i.e., three atoms) in common. The main constructions of this generalization of the Voronoi−Delaunay method are illustrated and compared to those of the original method in the right panel of Figure 1.

When the properties of the empty space are analyzed in terms of the Voronoi S-network in a system, the same sets of data are required as for the use of the classical Voronoi network.[34] Thus, the coordinates of the network sites should be kept in the array {D}, whereas their connectivity (i.e., the bonds of the network) is stored separately, in array {DD}. Because each bond determines the bottleneck between a pair of network sites, it is useful to have a special array $\{R_b\}$ containing the radii of the bottlenecks. The radii of the interstitial spheres, each of them corresponding to a network site, are stored in array $\{R_i\}$. The algorithm proposed by us[43] provides the values of $\{R_b\}$ and $\{R_i\}$ directly from the determination of the network. The information needed to conveniently work with the Delaunay S-simplexes, i.e., the lists of the atoms determining the network sites, is contained in the array {DA}. Finally, the array $\{V_e\}$, containing the values of the empty volume inside the Delaunay S-simplexes, provides the information needed to analyze the volume of the voids. These volumes can be calculated using the array {DA} together with the coordinates {A} and radii $\{R_a\}$ of the atoms of the system studied.

Some Peculiarities of the Voronoi S-Tessellation for Ensembles of Spheres. The Voronoi S-tessellation in systems of spheres of different sizes has, in general, some specific features that can hamper its use in the analysis of the interatomic space.[34] However, these features are usually not manifested in systems corresponding to physically sensible arrangements of molecules, and hence the methodology can directly be applied to most of the physical systems. Nevertheless, the peculiar features of the S-tessellation are absent from the classical Voronoi tessellation, which can make the analysis of the interatomic space difficult, and hence, the specific arrangements of the atoms corresponding to these peculiarities should be marked. These possible features of the Voronoi S-tessellation are discussed in detail elsewhere;[34,43] therefore only a brief summary of them is given here.

The main reason of the unpleasant peculiarities of the Voronoi S-tessellation is that, unlike in the case of the original Voronoi tessellation, the Voronoi surface dividing the space between two atoms is now a second-order curve (hyperboloid) rather than a plane. Therefore, some of the Voronoi S-regions can be principally different from a polyhedron. In particular, such regions can have only two faces, and hence no vertexes. More complex cases are discussed in detail elsewhere.[34] Such peculiarities are manifested if a small atom is located in a narrow gap between larger ones. This example shows that the Voronoi S-network can even be disconnected. In such cases it has to be found out how to connect separate parts of the Voronoi S-network. In the classical approach, the Voronoi network is singly connected and connects all the simplex cavities present in the system. Our experience shows that real molecular systems also possess singly connected Voronoi S-networks. Nevertheless, the singly connectivity of the S-network should be controlled in the stage of the network construction.[43]

Another possible peculiarity of the Voronoi S-network is that its two different sites can correspond to the same four atoms. In this case each site corresponds to its own interstitial sphere, and hence the corresponding Delaunay simplex contains two inscribed spheres. This peculiarity can, however, easily be taken into account in the analysis of the Voronoi S-network.

The next problem is that the Delaunay S-simplexes, unlike their classical analogues, can overlap each other in certain conditions. The existence of such "internal" S-simplexes introduces an error in the calculation of the volume of the interatomic voids. These simplexes can readily be distinguished when constructing the Voronoi S-network. However, specific atomic arrangements leading to this peculiarity appear with rather low probabilities in physically relevant disordered mo-

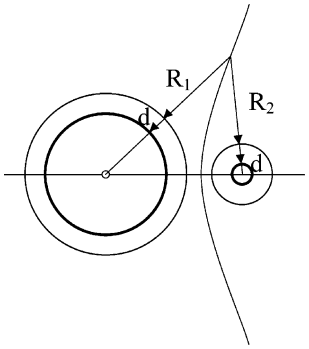

Figure 2. Illustration of the fact that the Voronoi S-network does not change if the radii of the balls (atoms) are decreased by the same value *d*.

lecular systems, and hence the above error is usually marginal. This can be verified by comparing the sum of the volumes of the calculated Delaunay S-simplexes with the total volume of the system. In the analyses presented in this paper the difference of the two volumes has always been found to be below 0.01%.

Consideration of Atomic Overlapping

Mathematically, the Voronoi S-network can be determined over the entire space, also inside overlapping atoms. However, when the interatomic space is analyzed, only the part of the network located outside the atoms has to be known. Hence, the problem of overlapping of the chemically bound atoms can easily be solved. By definition, each bond of the Voronoi S-network is the locus of points located at equal distance from the surfaces of the nearest three balls (atoms). This locus does not change if we change the radii of the corresponding balls by the same value *d* (see Figure 2). Similarly, the S-network site (i.e., the common vertex of the Voronoi S-regions) remains at the same position if the radii of the corresponding four balls are changed by the same value. This particular feature of the Voronoi S-tessellation allows the construction of a new, reduced system by decreasing the radii of all spheres of the initial system by a constant value *d* to avoid their overlapping. The Voronoi S-network of the system investigated can then be constructed on the reduced system of nonoverlapping balls. The data required to describe the S-network (i.e., the coordinates of network sites {D}, the table of connectivity {DD}, and the table of the incidence of sites and atoms {DA}) fully coincide for the initial and the reduced system. The values of the radii of the interstitial spheres $\{R_i\}$ and bottlenecks $\{R_b\}$ for the initial system are simply related to the corresponding values $\{R_i'\}$ and $\{R_b'\}$ of the reduced system as $R_i' = R_i + d$ and $R_b' = R_b + d$. Obviously, some of these values can be negative in the initial system, indicating that the corresponding sites or bonds are completely covered by the atomic spheres and hence can be neglected in the analysis. A similar procedure can be applied if only those regions of the interatomic space are of interest in which the radius of the bottlenecks exceeds a given limiting value and hence is accessible for a probe of this radius. The procedure of determining the part of the Voronoi S-network situated in the empty space between the atoms is illustrated in Figure 3.

Finally, it should be noted that although the above procedure proposed to avoid atomic overlapping by decreasing all the atomic spheres of the system is rather simple, it is not always feasible in this form. Obviously, the value of *d* cannot be smaller than the radius of the smallest atom of the system, whereas the system might contain large atoms, the overlapping of which exceeds *d*. This problem can be avoided by reducing the size

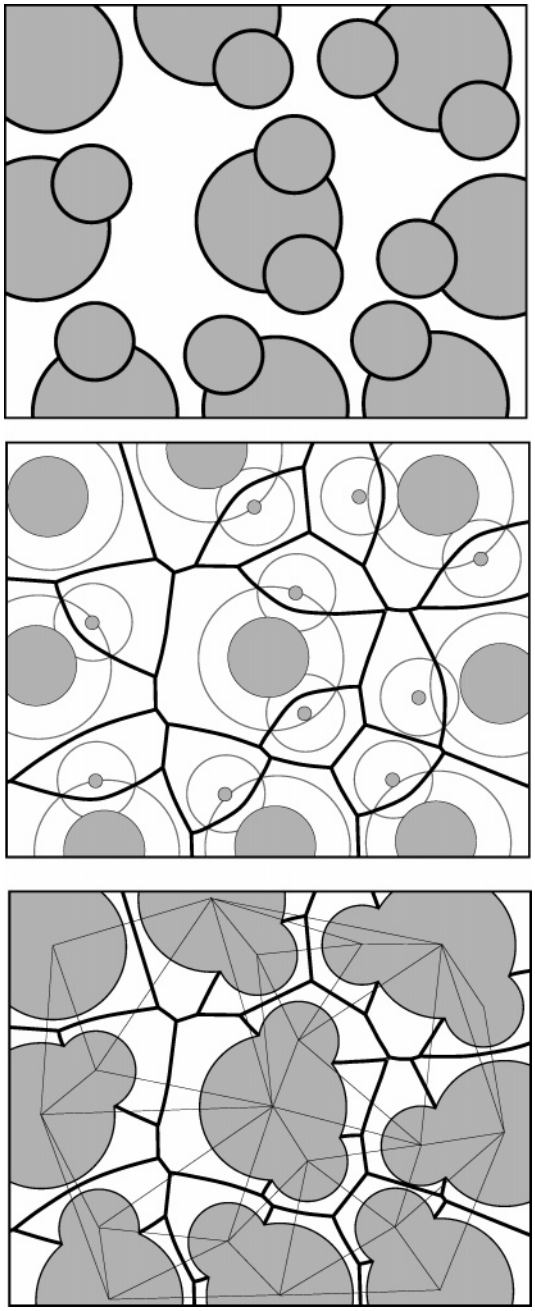

Figure 3. Two-dimensional illustration of the determination of the Voronoi S-network and Delaunay S-simplexes in a molecular system. Top: the system to be analyzed, represented as an ensemble of partly overlapping balls of different radii. Middle: reduced system, obtained by decreasing the radii of all of the balls by the same value *d*. The Voronoi S-network obtained in the reduced system is also shown (thick lines). Bottom: parts of the Voronoi S-network located outside the atomic spheres (thick lines) and Delaunay S-simplexes (thin lines) of the system.

of the atomic spheres locally, i.e., when a given site of the S-network is calculated, only the overlapping of the corresponding four atoms is eliminated.[43] Overlapping cannot be eliminated when one of the atoms is located fully inside another one. However, this case is of no practical interest, because the internal atom does not participate at all in the formation of empty interatomic space and thus can be neglected.

Determination of the Interatomic Voids

The empty space in a three-dimensional system of atoms is a complex, singly connected region confined by the atomic

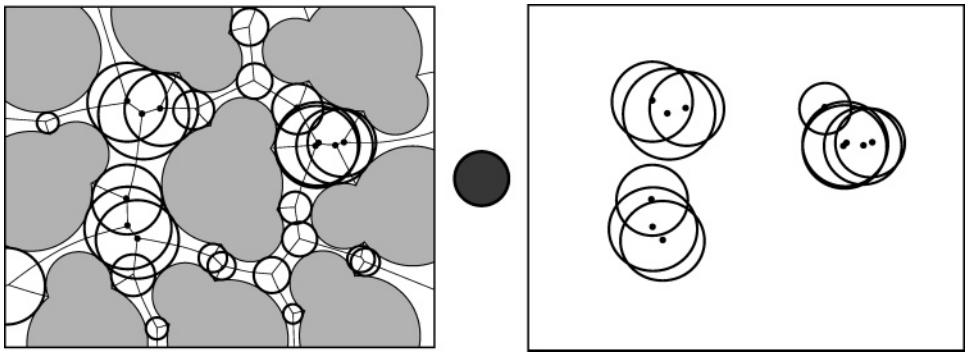

Figure 4. Two-dimensional illustration of the R_i coloring of the Voronoi S-network sites in the system shown in Figure 3. Left: all interstitial spheres of the system. Black dots indicate the Voronoi S-network sites corresponding to interstitial spheres larger than the probe shown between the two figures. Right: interstitial spheres having a radius larger than that of the probe.

surfaces. Any interatomic void to be distinguished is a part of it and depends on the detection criterion. A natural physical way of defining voids is through the value of the radius of a probe (test sphere) that can be put in the given void. Thus, voids are the parts of the interatomic space that are accessible for a given probe. Therefore, when voids are discussed, the radius R_{probe} of the corresponding probe should always be indicated. The number, size, and morphology of the voids in a given system depend on the probe radius: though almost the whole empty interatomic space is accessible for a small probe, only the most spacious cavities represent voids for larger ones.

Interstitial Spheres (R_i Coloring). Interstitial spheres are simple but important elements of the empty interatomic space. As has been discussed in a previous section, these spheres represent real empty volume between the atoms. Therefore, the values of their radii indicate the length scale of the voids present in the system. Because each site of the Voronoi S-network is the center of one of these spheres, once the coordinates of the network sites {D} as well as the radii of the interstitial spheres $\{R_i\}$ are known, the location of the large and small voids can readily be determined. For example, the largest voids can simply be distinguished by marking (coloring) the S-network sites the corresponding interstitial spheres of which have a radius larger than a limiting value R_{lim}. This procedure of distinguishing the sites of the Voronoi S-network by the radius of the corresponding interstitial spheres, called the R_i coloring the network,[34,50] is illustrated in Figure 4.

System of Bottlenecks. Determination of Voids (R_b Coloring). A more comprehensive analysis of the voids and interatomic channels requires also the consideration of the bottlenecks of the empty space, i.e., the bonds of the Voronoi S-network. If a probe can move along an S-network bond (i.e., pass through a bottleneck) then both of the network sites connected by this bond are also accessible for it.[34] Thus, the regions accessible for a given probe can be determined by distinguishing the bonds, the bottleneck radius of which exceeds a given limiting value. The clusters consisting of these bonds represent the fairways of the empty interatomic regions along which a given probe can be moved. Distinguishing bonds of the Voronoi S-network according to their bottleneck radii is called the R_b coloring of the network.[34,51] The use of the R_b coloring of the Voronoi S-network in determining the voids in a system is illustrated in Figure 5.

The description of the voids as clusters of S-network bonds and sites is very useful in locating the large voids in the system investigated. However, when a more detailed analysis of the voids is done, their volumes should also be calculated. This can be done with the help of the Delaunay S-simplexes. Knowing the sites of the Voronoi S-network that are involved in a given cluster, all S-simplexes composing this void are also known (see Figure 5b). Whilst the cluster of the S-network sites and bonds represents the "skeleton" of a void, the union of the empty volumes of the corresponding S-simplexes form its "body" (see Figure 5c). The void is confined by the surfaces of the atomic spheres and flat faces of the corresponding S-simplexes; and the probe can move along the S-network bonds between the sites involved in this void. The rest of the empty space in the system is inaccessible for this probe. The proposed representation of the voids provides a quantitative basis for the analysis of various characteristics of them.

Calculation of the Empty Space of the Delaunay S-Simplex. As shown in the previous subsection, in determining the volume of the voids present in a system the volume of the empty part of the corresponding S-simplexes has to be calculated. At first glance, it seems to be a rather straightforward task; the volume to be determined is simply the total volume of the simplex minus the volume occupied by the parts of its own atoms. This calculation is based on the assumption that only the atoms determining an S-simplex can occupy any part of its volume. However, besides their own atoms, S-simplexes often involve several alien atoms as well.[34,52] The volume occupied by these atoms in an S-simplex is rather difficult to take into account. Additional problems arise from the overlapping of atoms inside the simplexes, which should also be taken into account to calculate the empty volume correctly. Although analytical formulas can be derived for treating double and triple overlapping, multiple overlapping, which appears rather often for the alien atoms, is analytically almost untreatable. Due to these difficulties, numerical calculation of the empty volume of an S-simplex is, in general, far more efficient and accurate than its analytical determination. Such a calculation can simply be done by filling the simplex by sample points (arranged either randomly or along a grid) and determining the fraction of points located outside the atoms. This procedure can be done rather efficiently, because the list of the alien atoms potentially overlapping with the simplex can be readily defined beforehand, using the Voronoi S-tessellation of the system. Namely, the distance of these atoms from the Voronoi S-network site corresponding to the S-simplex considered cannot be larger than $R_{sph} + R_{max}$, where R_{sph} is the radius of the sphere inscribed among the atoms determining the S-simplex, and R_{max} is the radius of the largest atom present in the system. The accuracy of the calculation can be improved by increasing the number of the test points used, which, however, increases also the computational cost of the calculation. In the analyses reported in the present paper these calculations have been done with an average accuracy of $\pm 2\%$.

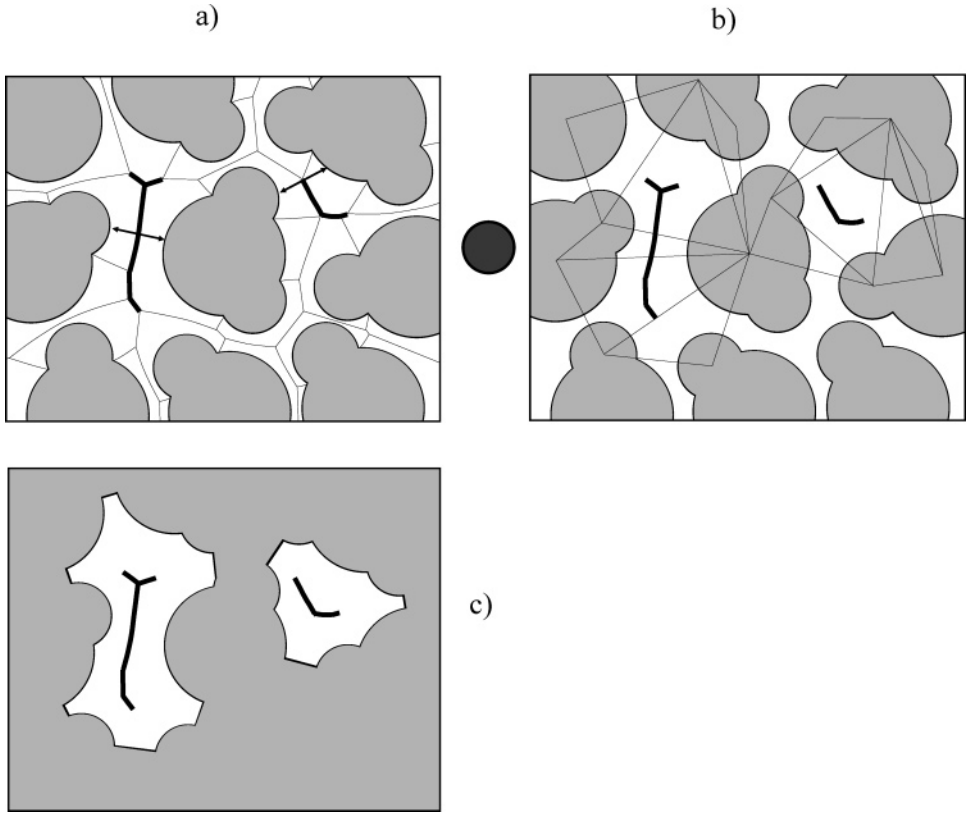

Figure 5. Two-dimensional illustration of the R_b coloring of the Voronoi S-network sites in the system shown in Figure 3. Thick lines indicate the bonds of the Voronoi S-network, the bottleneck radius of which exceeds the radius of the probe shown between the two top figures. Top left: parts of the Voronoi S-network located outside the atomic spheres. The location of the bottleneck along two selected bonds is shown by arrows. Top right: detected clusters of R_b-colored S-network bonds, and the corresponding Delaunay S-simplexes. Bottom: voids corresponding to the clusters of R_b-colored S-network bonds.

Properties of Voids in the Simulated DMPC Membrane

The detailed investigation of the properties of voids is of particular interest in hydrated membranes formed by ampiphilic lipid molecules. These membranes, consisting of hydrophobic and hydrophilic regions as well as an aqueous phase hydrating the lipid molecules are highly anisotropic and inhomogeneous systems, and hence the voids present in such systems are expected to show a rather complex behavior. The characteristics of these voids influence the properties of the membranes in several respects. Thus, the diffusion of small molecules in the membrane, and hence the permeability of the membrane depend strongly on the size, shape, and orientation of its voids. Because phospholipid molecules, such as DMPC and DPPC are the main components of the membranes of eukaryotic cells, the membranes built up by such molecules are also of biological relevance; any investigation of the structure and function of the real biological membranes of rather complex structures requires detailed understanding of the properties of simple phospholipid membranes. Although phospholipid membranes have been intensively studied by computer simulation methods,[45−49,53−62] the properties of the voids in such membranes have been the subject of only a few studies, focusing primarily on the distribution of the empty space across the membrane.[45,47−49]

System Investigated. The system investigated in the present study is a computer model of the fully hydrated DMPC bilayer, as obtained from a recent all-atom Monte Carlo simulation, performed on the isothermal−isobaric (N,p,T) ensemble under physiological conditions (i.e., at 1 atm and 310 K).[61] Each of the two membrane layers contain 25 DMPC molecules, described by the CHARMM22 force field optimized for proteins and phospholipid molecules,[63] and the bilayer is hydrated by 2033 TIP3P[64] water molecules. The bond lengths and bond angles of the molecules are fixed at their equilibrium values, whereas torsional flexibility of the DMPC molecules is introduced. The sample analyzed here consists of 1000 independent configurations, each of them separated by 10^5 new Monte Carlo steps from the previous one. Details of the simulation of the system and a thorough analysis of its molecular level structure are given in our previous papers.[48,61,62] The snapshot of an instantaneous sample configuration of the system is shown in Figure 6.

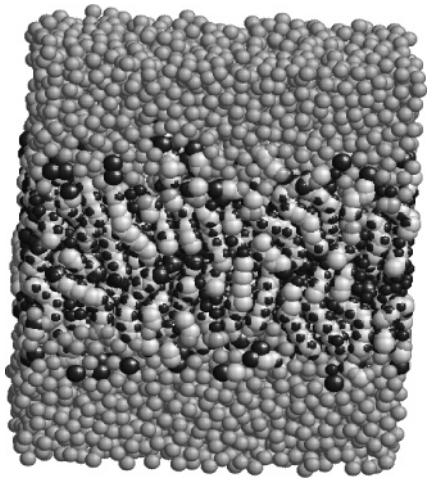

Figure 6. Snapshot showing an equilibrium configuration of the atoms in a simulated fully hydrated DMPC bilayer.

Main Characteristics of the Interatomic Space. *R_i Distribution.* As mentioned above, the length scale of the voids in a

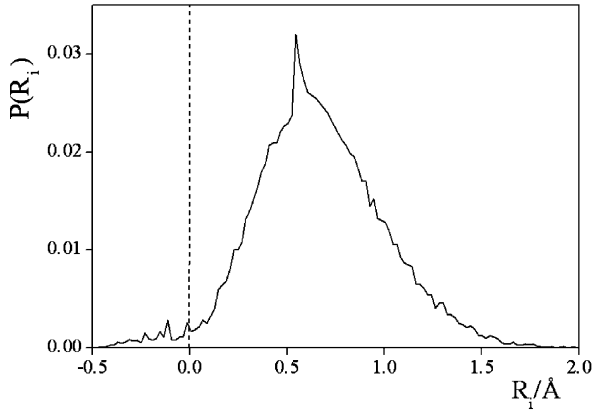

Figure 7. Distribution of the radii of the interstitial spheres R_i present in the simulated fully hydrated DMPC bilayer. Negative values of R_i correspond to the regions completely covered by the atoms.

system is set by the radii of the interstitial spheres. Figure 7 shows the distribution of the radii of these spheres R_i in the lipid bilayer simulated. As is seen, the distribution is rather symmetric; it is not extended above 1.8 Å, indicating that the system does not contain particularly large voids. The highest fraction of the interstitial spheres has a radius of about 0.6 Å, indicating that the bilayer studied is a rather dense system. It should be noted that the negative R_i values are assigned to the interstitial spheres of the reduced model, which, after acquiring the initial atomic sizes, appear completely inside the atoms, as discussed in a previous section. Real voids correspond to the positive R_i values. The sharp peak appearing between 0.5 and 0.6 Å at the position of the main broad peak of the distribution is due to the intramolecular voids of DMPC molecules (i.e., to the spheres inscribed between the atoms belonging to the same molecule).

Spatial Distribution of the Interstitial Spheres. Figure 8 shows the interstitial spheres, the radii of which exceed 1.6 and 1.2 Å, respectively, in the sample configuration shown in Figure 6. The use of the former limiting radius value leads to the few large voids of the system (see Figure 7), whereas with the choice of $R_i > 1.2$ Å a number of smaller voids are also detected. Both choices of R_i demonstrate that the population of large voids is considerably higher at the center of the bilayer and in the aqueous phase than in the region of hydrophilic headgroups of the DMPC molecules, where only a few large voids can be detected. This observation is in accordance with the fact that the density profile of the system goes through a clear maximum in the region of the lipid headgroups.[61]

Fraction of the Empty Space across the Membrane. The qualitative conclusions drawn from the snapshots of Figure 8 on the distribution of the empty space along the membrane normal can be quantified by calculating the profile of the fraction of the empty volume across bilayer. This profile can be calculated in several different ways, even without using the Voronoi−Delaunay method (e.g., by placing sample points in the system either randomly or along a grid, as done by Marrink et al.[49]). However, having already determined the Voronoi S-network and the Delaunay S-simplexes of the system, the profile can readily be calculated. Thus, the empty volume in a given slice of the system along the membrane normal axis z can be estimated as the sum of the empty volumes of the Delaunay S-simplexes located in this layer. The position of an S-simplex can simply be estimated as the position of the corresponding Voronoi S-network site (i.e., the total empty volume of an S-simplex is assigned to the membrane layer in which the corresponding S-network site is located). This approach assumes that the characteristic size of the Delaunay S-simplexes of the system is considerably smaller than the length of the edge of the basic box along which the profile is calculated. This condition is safely satisfied in the case of the system analyzed here.

The obtained profile of the fraction of empty space, symmetrized over the two sides of the membrane, is shown on the top panel of Figure 9. Following the convention used in our previous paper,[65] the system is divided into three separate regions in the following analyses. Thus, region 1 is located at the middle of the membrane, at $|z| \leq 8$ Å ($z = 0$ being in the middle of the bilayer); region 2 covers the layer at 8 Å $\leq |z| \leq$ 24 Å, whereas region 3 is located farthest from the membrane interior, at $|z| \geq 24$ Å. These regions roughly coincide with the apolar hydrocarbon phase of the bilayer, the region of the hydrophilic headgroups of the DMPC molecules, and the region of bulklike water, respectively.[61] As is seen, the largest fraction (almost 50%) of the space is found to be empty in the aqueous phase of the system, whereas the fraction of the empty space is clearly the smallest in the regions of the hydrophilic DMPC headgroups, being as low as 30% in the middle of this region. The obtained profile is in good agreement with the similar profile estimated by Marrink et al. in the hydrated bilayer of DPPC by setting a grid of sample points in their system.[49]

The above approach can readily be used to calculate also the *partial* profiles of the fraction of empty volume (in which only the volume belonging to large enough voids is taken into account) across the system. Such profiles can simply be determined by considering only the Delaunay S-simplexes the

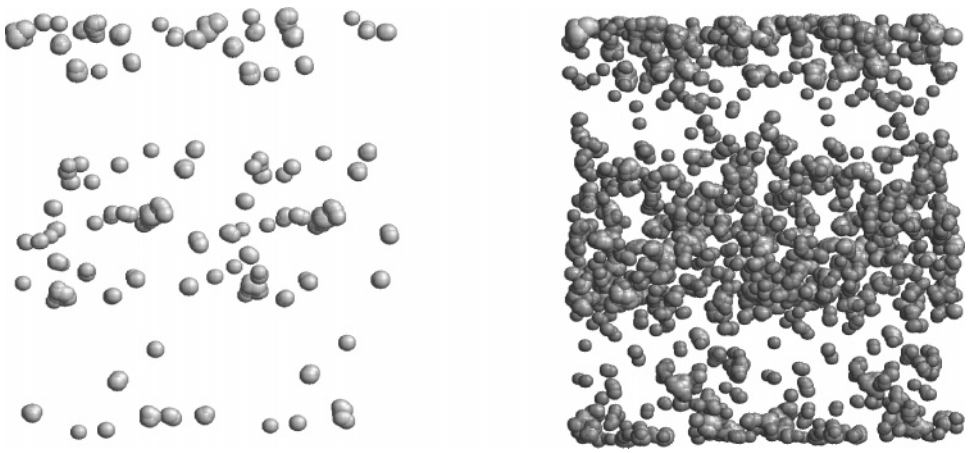

Figure 8. Interstitial spheres of a radius of at least 1.6 Å (left) and 1.2 Å (right) in the configuration shown in Figure 6.

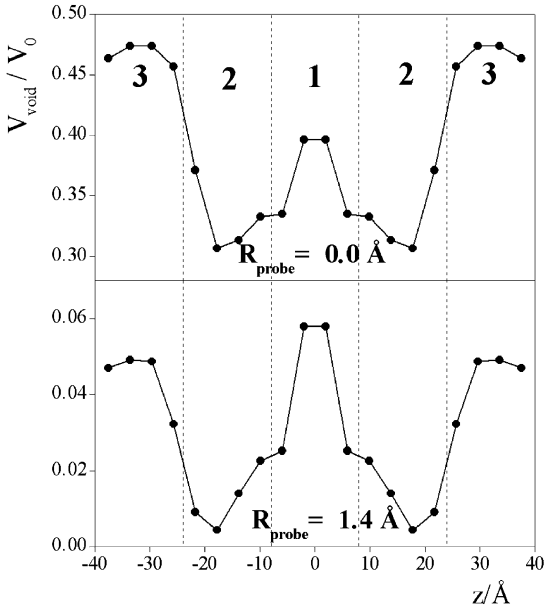

Figure 9. Profile of the fraction of the empty space (top), and partial profile of the fraction of the empty space assigned to voids accessible for a probe of the radius of 1.4 Å (bottom) across the simulated fully hydrated DMPC membrane. The dashed vertical lines indicate the division of the membrane into three separate regions.

radius of the interstitial sphere of which is larger than a limiting value. The partial profile obtained with the limiting radius value of $R_{probe} = 1.4$ Å is shown on the bottom panel of Figure 9. As is seen, contrary to the total empty volume, the highest fraction of the space belongs in region 1 to voids accessible for a probe of this size. This finding, being also in qualitative agreement with the results of Marrink et al.,[49] indicates that the empty space is distributed among a large number of rather small cavities in the aqueous phase, and among a few more spacious cavities in the middle of the membrane.

Interatomic Cavities as Clusters on the Voronoi S-Network. The voids accessible for relatively large probes in a system are of particular interest, as they form the widest channels and pores. As discussed in a previous section, these voids can be revealed by means of the R_b coloring of the Voronoi S-network of the system, in which the bonds whose bottleneck radius exceed a given limiting value of R_{probe} are distinguished. For large values of R_{probe} the procedure results in a small number of isolated clusters of the bonds, corresponding to the most spacious voids of the system. Considering also some narrower bottlenecks (i.e., decreasing the value of R_{probe}) more complex clusters are obtained. At a critical value of the probe radius the system of the clusters becomes percolated; i.e., a large cluster extending over the entire system arises, through which the probe can pass from any part to any other part of the system. Finally, when R_{probe} is zero, all the bonds of the Voronoi S-network located in the empty space of the system are colored. Obviously, the sites of the Voronoi S-network connecting contiguous bonds are also involved in the cluster, because any probe that can pass along an S-network bond fits also into the interstitial spheres at both terminal sites of the bond. To find all places accessible for a given probe in the system, the single sites of the Voronoi S-network at which the radius of the interstitial sphere exceeds the radius of the probe should also be taken into account, even if the bottleneck radii of all the bonds emanating from this site are smaller than this limiting value. Such voids consist of one single simplex only. Note that once the clusters accessible for the probe of a given size are distinguished by the R_b coloring procedure, and the single sites with the proper interstitial sphere are also taken into account, the properties of the Voronoi S-tessellation guarantee that the system does not contain any other void accessible for this probe.

Figure 10 shows the bonds of the Voronoi S-network whose bottleneck radius exceeds 1.3 Å in the sample configuration shown in Figure 6. Similarly to the interstitial spheres revealed by the R_i coloring of the system (see Figure 8), most of the S-network bond clusters representing the voids are also located in the aqueous phase and in the middle of the membrane. Nevertheless, the information extracted from the R_b coloring of the S-network differs from that provided by its R_i coloring, even if the clusters distinguished by the two methods almost coincide for large enough probes.

As seen from Figure 10, the use of the probe radius of 1.3 Å leads to a number of small clusters that are separated from each other; the probe can fit into any of the corresponding voids but cannot move from one void to another. To determine the critical probe radius R_{crit} at which the system of clusters becomes percolated, we have repeated the R_b coloring procedure by systematically decreasing probe radii. Due to the anisotropy of the system, however, the value of R_{crit} differs when the clusters are percolating only in lateral directions (i.e., along the *x* and *y* axes) from the value describing percolation even along the membrane normal axis *z*. For the lateral percolation we have obtained the value of $R_{crit} = 0.803 \pm 0.016$ Å, whereas for the complete percolation (i.e., also along the membrane normal axis) the much smaller critical probe radius value of $R_{crit} = 0.650 \pm$

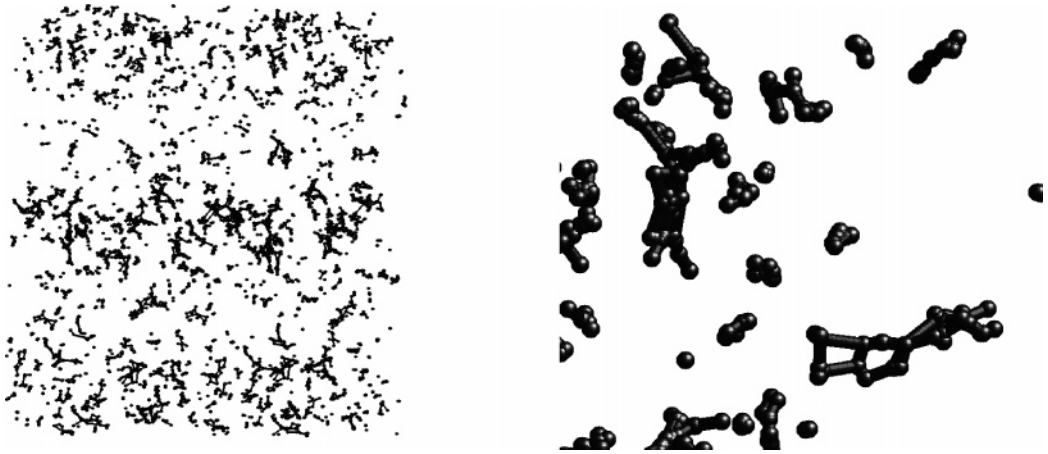

Figure 10. Right: clusters of the Voronoi S-network bonds having a bottleneck radius of at least 1.3 Å in the configuration shown in Figure 6. Left: a fragment of this picture shown on an enlarged scale.

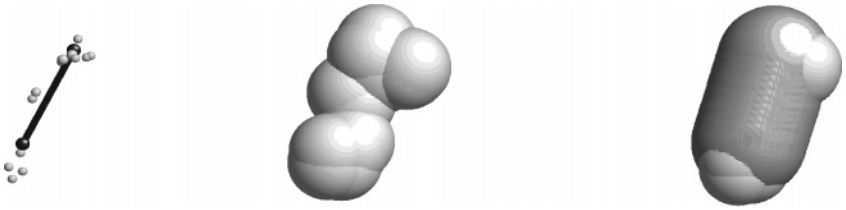

Figure 11. Illustration of the construction of the spherocylinder representing a given void. Left: the cluster of the Voronoi S-network sites representing the void. The principal axis of the tensor of inertia of these sites is also indicated (see the text). Center: union of the interstitial spheres centered on the sites. Right: the obtained spherocylinder (drawn on the top of the interstitial spheres).

0.014 Å has resulted. This rather large difference between the two critical radii is due to the fact that the region of the hydrated DMPC headgroups is rather dense, and hence it contains fewer and smaller voids than the other regions of the system. To exclude the influence of the headgroup region, we have also calculated the critical probe radius for the cluster percolation along the membrane normal in the central membrane region of the hydrocarbon lipid tails (i.e., region 1). The obtained value of $R_{crit} = 0.892 \pm 0.089$ is now even slightly larger than the value corresponding to the lateral percolation. However, it is worth noting that all these critical radii are much smaller than the size of the smallest molecules, indicating that the DMPC bilayer does not contain readily formed channels along which any penetrant molecule could pass through the membrane. Therefore, the mechanism of the cross-membrane diffusion of small molecules involves the interaction between the penetrant and the lipid molecules, as the penetrant can only move into voids created in the membrane due to the thermal motion of the lipids and to the lipid−penetrant interaction, i.e., it has to push apart the lipid molecules to make its way through the membrane.

Analysis of the Void Shape. In our previous paper,[65] we have proposed to represent the determined interatomic voids as spherocylinders. In finding the spherocylinders covering the voids, optimally fitting procedures have been found to be rather time-consuming. Therefore, a method for the direct determination of the parameters describing the spherocylinders has been proposed.[65] Here we briefly recall the main points of this method. A fictitious "mass" proportional to the empty volume of the corresponding Delaunay S-simplex is assigned to each site of the S-network cluster representing the void. In this way the voids of any complex shape are represented by a system of massive points. Then the tensor of inertia of the void is calculated using these fictitious masses. The axis of the tensor along which its principal value is minimal indicates the direction of the largest extension of the void and is taken as the axis of the required spherocylinder. The lengths of the cylindrical part of the spherocylinder L are calculated by projecting all the sites of the cluster to this axis, and the mean square deviation of these projections is calculated from the fictitious center of mass of the cluster. Finally, the radius of the spherocylinder R is unambiguously determined by the condition that the volume of the spherocylinder should be equal to that of the void:

$$V_{void} = R^2\pi\left(L + \frac{4}{3}R\right) \tag{1}$$

where the volume of the void V_{void} is the sum of the empty volumes of the composing Delaunay S-simplexes (i.e., the total fictitious mass of the cluster). This procedure is illustrated in Figure 11.

To characterize the size, shape, and orientation of the voids present in the hydrated DMPC bilayer, we have calculated the volume of the corresponding spherocylinder V_{void}, the parameter α characterizing the sphericity of the void, defined as

$$\alpha = \frac{2R}{2R + L} \tag{2}$$

and the cosine of the angle γ formed by the axis of the spherocylinder and the bilayer normal axis z, respectively. The value of the parameter α varies from zero (for infinitely long spherocylinders) to unity (for perfect spheres). To avoid the arbitrariness of the void definition due to the choice of the probe radius R_{probe}, we have calculated the above parameters with seven different probe radii, starting from $R_{probe} = 1.0$ Å and increasing the probe radius up to 1.6 Å by a step of 0.1 Å. This range of R_{probe} covers the descending side of the peak of the $P(R_i)$ distribution (see Figure 7), and hence only the relatively large voids of the system can be detected in this way. Furthermore, voids of this size can be relevant for accommodating a water molecule, because similar values are thought to be realistic as the effective water radius in polar biomolecular interactions.[66,67] The mean values of V_{void}, α, and cos γ have been determined in the three membrane regions separately. The dependence of the obtained average values on the probe radius in the three regions is shown in Figure 12. As is seen, all the three characteristics of the voids presented are noticeably different in the three regions of the bilayer. It should also be noted that the relation of the mean values of the parameters obtained in the different membrane regions is preserved for all probe sizes used; i.e., the results are stable to the void detection criterion. Similar behavior has also been observed for several other void characteristics[65] (e.g., the length L and radius R of the spherocylinders) that are not presented here.

The results obtained for the mean volume of the voids are in accordance with the qualitative picture seen from Figures 8 and 10. Thus, the largest voids are clearly found to be located in the central part of the membrane, whereas the voids located at the region of the hydrated lipid headgroups are, on average, considerably smaller than those in the other parts of the membrane. It should be noted that, despite the above results, the fraction of the empty space is found to be considerably smaller in the apolar region of the membrane than in the region of bulklike water (see Figure 9), indicating that the empty space is distributed in a considerably more ordered way among the hydrocarbon chains of the DMPC molecules than in the aqueous phase. This conclusion is also in accordance with the fact that the voids in region 1 are, on average, considerably less spherical than in region 3.

It is also seen that though the obtained $\langle V_{void}\rangle(R_{probe})$ curve is monotonic in regions 2 and 3, it goes through a minimum in the region of the membrane interior. The reason of this behavior is the fact that the decrease of the probe radius, simultaneously with the appearance of small voids, leads also to the fusion of the voids that are separated for larger probe radii after a certain point. Obviously, this fusion of the separated voids appears at smaller probe radii values in systems containing smaller voids.

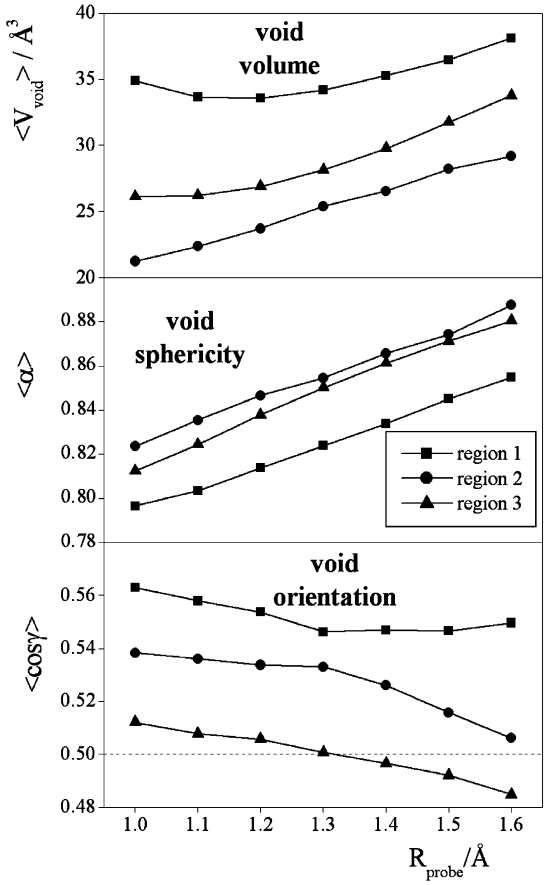

Figure 12. Dependence of the mean volume of the voids (top), mean value of the sphericity parameter α of the spherocylinders representing the voids (middle), and mean cosine of the angle γ formed by the axis of the spherocylinder and the membrane normal axis z on the radius of the probe used in the void detection criterion (R_{probe}) in the three separate membrane regions: squares, region 1 (hydrocarbon tails); circles, region 2 (hydrophilic headgroups); triangles, region 3 (aqueous phase).

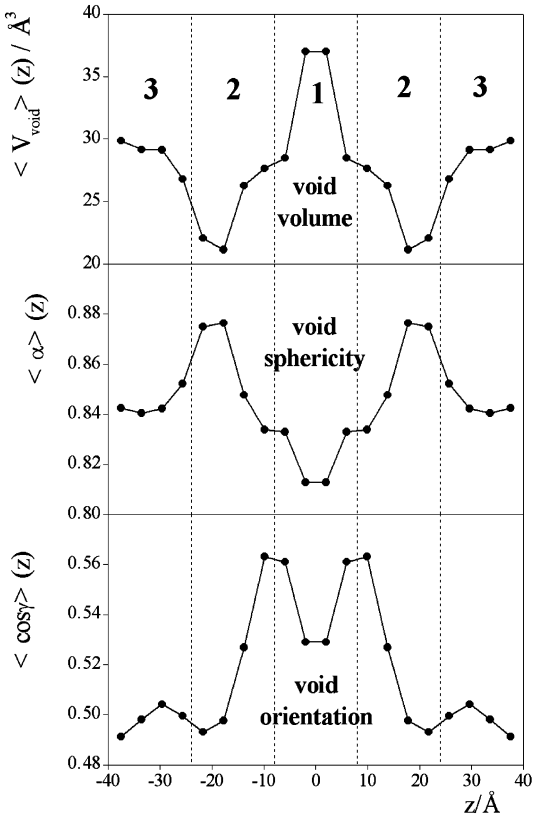

Figure 13. Profile of the average volume (top), sphericity parameter (middle), and orientation (bottom) of the spherocylinders representing the voids across the simulated fully hydrated DMPC bilayer. The dashed vertical lines indicate the division of the membrane into three separate regions.

Therefore, the minimum behavior of the $\langle V_{void} \rangle (R_{probe})$ curve can also be expected in regions 2 and 3 at R_{probe} values below 1.0 Å. Indeed, traces of the presence of such a minimum can already be seen on the curve obtained in region 3 below about 1.2 Å.

In analyzing the average orientation of the voids it should be noted that the angle γ can vary between 0° and 90°, and hence the value of cos γ scatters between 0 and 1. Thus, isotropic orientation of the voids corresponds to the $\langle \cos \gamma \rangle$ value of 0.5 (indicated by a dashed horizontal line in Figure 12). The $\langle \cos \gamma \rangle$ values larger than 0.5 indicate that the preferred orientation of the voids is perpendicular rather than parallel to the plane of the bilayer, whereas $\langle \cos \gamma \rangle < 0.5$ indicates opposite orientational preferences. The strongest orientational ordering of the voids is seen in the middle region of the membrane for all the probe radii used. Here the voids are aligned preferentially parallel with the bilayer normal, and hence, also with the C−C bonds of the lipid hydrocarbon tails.[61] The fusion of the voids with decreasing probe radius makes this orientational preference even stronger, as the obtained $\langle \cos \gamma \rangle (R_{probe})$ function increases monotonically with decreasing probe radius below 1.3 Å. A similar but weaker orientational preference of the voids is seen in the region of the headgroups, in accordance with our previous finding that the preference of the lipid headgroups themselves for a parallel orientation with the membrane normal axis z is also considerably weaker than that of the hydrocarbon lipid tails.[61] Finally, the orientation of the voids located in the aqueous phase is nearly isotropic, although a slight but deliberate change of $\langle \cos \gamma \rangle$ is seen with changing probe radius. This dependence of $\langle \cos \gamma \rangle$ on R_{probe} in region 3 is rather similar to that in region 2, indicating that the likely reason is simply that the definition of the separate membrane regions used here is rather arbitrary, and hence, due to the roughness of the membrane surface, parts of the headgroups of several lipid molecules can also be located in region 3, influencing the properties of the voids also in this region. Although this influence is usually rather small, it becomes evident when it induces a slight orientational order among the voids otherwise oriented in a totally disordered way.

To analyze the change of the void characteristics along the membrane normal axis z in more detail, we have calculated the profile of $\langle V_{void} \rangle$, $\langle \alpha \rangle$, and $\langle \cos \gamma \rangle$ across the membrane using the R_{probe} value of 1.3 Å. The position of a void is defined by the fictitious center-of-mass of the corresponding S-network cluster. The obtained profiles, symmetrized over the two sides of the bilayer, are shown in Figure 13. The void volume profile is in clear accordance with the density profile of the membrane,[61] higher densities always correspond to the presence of smaller voids on average. The only deviation from this correspondence is that the peak of the $\langle V_{void} \rangle (z)$ profile at the middle of the membrane is noticeably sharper than the density minimum in this region (see Figure 4 of ref 61). This deviation indicates again that the empty space is considerably more ordered in the middle of the membrane than in its outer parts. The comparison of the obtained $\langle V_{void} \rangle (z)$ and $\langle \alpha \rangle (z)$ profiles shows that there is a clear and strong correlation between the average size and sphericity of the voids; i.e., larger voids are, on average, consistently less spherical than smaller ones. Thus, the most spherical voids are located in the dense region of the headgroups.

This result is in clear accordance with the conclusion drawn in a previous study[48] from the comparison of the probability profile of finding spherical cavities of a given minimum size and the density profile of the system, even if the difference in sizes of the atoms constituting the system has not been taken into account in that study.[48]

The orientational profile of the voids shows a clear peak at about $z = \pm 8$ Å, i.e., where approximately the outer part of the hydrocarbon lipid tails is located.[61] This peak is followed by a minimum in the middle of the memrane, i.e., among the hydrocarbon chain terminal groups. This difference observed between the orientational ordering of the voids in the outer and inner part of the region of the hydrocarbon tails is in agreement with the findings of Marrink et al. on the difference between the orientational ordering of the lipid tails themselves[45,46,49] and indicates again that the orientational ordering of the voids is clearly induced by that of the chains of the DMPC molecules in the membrane.

Summary and Conclusions

In the present work a generalized version of the Voronoi−Delaunay method is used to analyze voids in a computer model of a hydrated lipid bilayer. The original method is modified to make it applicable for molecular systems, i.e., ensembles of partly overlapping spheres of different sizes, as well. Thus, the Voronoi region of the atoms is confined by second-order surfaces, being the locus of spatial points located equally far from the surface rather then the center of the central atom and its corresponding neighbor. The Voronoi S-network, constructed in this way, is a map of the voids confined between the atoms, whereas the Delaunay S-simplexes determine the simplest interatomic cavities that can be used to represent any complex intermolecular void.

The applicability of the generalized version of the method is clearly demonstrated by performing a detailed analysis of the intermolecular voids in a simulated model of the fully hydrated DMPC bilayer. In analyzing the properties of voids that are accessible for probes of different sizes, we have found that the voids of the system form a percolating network across the system only for probe sizes significantly below the size of the smallest molecules, indicating that the membrane does not contain any preexisting channels along which small penetrants can pass through the membrane. The properties of the voids are found to be significantly different in the hydrocarbon phase and headgroup region of the membrane as well as in the aqueous phase. The largest and most elongated voids are found to be in the hydrocarbon phase. The comparison of the preferred orientation of these voids with that of the lipid tails[45,46,49,61] reveals a clear correlation between them. Thus, they prefer the parallel alignment with the membrane normal axis, and this preference is found to be considerably stronger in the outer part of the region of the lipid tails. A correlation between the size and shape of the voids is also observed, namely smaller voids are found to be, on average, more spherical. In accordance with our previous results,[48] the smallest and most spherical voids are found to be in the dense region of the hydrated lipid headgroups. The fraction of the empty space is found to be largest in the aqueous phase, although considerably more large cavities are found to be in the hydrocarbon phase. This finding, in accordance with previous results,[49] indicates that the empty space is distributed considerably more uniformly (i.e., among more cavities of smaller size) in the aqueous than in the hydrocarbon phase.

Acknowledgment. This work has been supported by INTAS under project No. 2001-0067, Russian Foundation for Fundamental Research under project No. 01-03-32903, Hungarian OTKA Foundation under project No. F038187, and the U.S. CRDF award No. NO-008-X1. P.J. is a Békésy György fellow of the Hungarian Ministry of Education, which is gratefully acknowledged.

References and Notes

(1) Voronoi, G. F. *J. Reine Andew. Math.* **1908**, *134*, 198.
(2) Delaunay, B. N. *Proc. Math. Congr. Toronto Aug 11−16 1924* **1928**, 695.
(3) Bernal, J. D. *Proc. R. Soc. London* **1964**, *A280*, 299.
(4) Finney, J. L. *Proc. R. Soc. London* **1970**, *319*, 479.
(5) Finney, J. L. *Proc. R. Soc. London* **1970**, *319*, 495.
(6) Hsu C. S.; Rahman, A. J. *J. Chem. Phys.* **1979**, *70*, 5234.
(7) Hsu C. S.; Rahman, A. J. *J. Chem. Phys.* **1979**, *71*, 4974.
(8) Hiwatari, Y.; Saito, T.; Ueda, A. *J. Chem. Phys.* **1984**, *81*, 6044.
(9) Medvedev, N. N.; Naberukhin, Y. I. *J. Non-Cryst. Solids* **1987**, *94*, 402.
(10) Oger L.; Gervois, A.; Troadec, J. P.; Rivier, N. *Philos. Mag. B* **1996**, *74*, 177.
(11) Brostow, W.; Chybicki, M.; Laskowski, R.; Rybicki, J. *Phys. Rev. B* **1998**, *57*, 13448.
(12) Medvedev, N. N.; Naberukhin, Y. I. *J. Phys. A* **1988**, *21*, L247.
(13) Medvedev, N. N.; Geiger, A.; Brostow, W. *J. Chem. Phys.* **1990**, *93*, 8337.
(14) Wilson M.; Madden, P. A. *Phys. Rev. Lett.* **1998**, *80*, 532.
(15) Bryant S.; Blunt, M. *Phys. Rev. A* **1992**, *46*, 2004.
(16) Thompson, K. E.; Fogler, H. S. *AIChE J.* **1997**, *43*, 1377.
(17) Voloshin, V. P.; Medvedev, N. N.; Fenelonov, V. B.; Parmon, V. N. *J. Struct. Chem.* **1999**, *40*, 681 (in Russian).
(18) Liao, Y. C.; Lee, D. J.; He, P. J. *Powder Techn.* **2002**, *123*, 1.
(19) Yang, R. Y.; Zou, R. P.; Yu, A. B. *Phys. Rev. E* **2002**, *65*, 041302.
(20) Voloshin, V. P.; Beaufils, S.; Medvedev, N. N. *J. Mol. Liq.* **2002**, *96−97*, 101.
(21) Malenkov, G. G. *Physica A* **2002**, *314*, 477.
(22) Angelov, B.; Sadoc, J. F.; Jullien, R.; Soyer, A.; Mornon, J. P.; Chomilier, J. *Proteins* **2002**, *49*, 446.
(23) Richards, F. M. *J. Mol. Biol.* **1974**, *82*, 1.
(24) Gavrilova M.; Rokne, J. *Int. J. Comput. Math.* **1997**, *61*, 49.
(25) Telley H.; Liebling, T. M. *Philos. Mag. B* **1996**, *73*, 395.
(26) Gellatly B. J.; Finney, J. L. *J. Non-Cryst. Solids* **1982**, *50*, 313.
(27) Mezei, M. *Mol. Simul.* **1988**, *1*, 327.
(28) Oger, L.; Richard, P.; Troadec, J. P.; Gervois, A. *Eur. Phys. J. B* **2000**, *14*, 403.
(29) Medvedev, N. N. *Dokl. Akad.. Nauk* **1994**, *337*, 767 (in Russian).
(30) Anishchik S. V.; Medvedev, N. N. *Phys. Rev. Lett.* **1995**, *75*, 4314.
(31) Okabe, A.; Boots, B.; Sugihara, K. *Spatial Tessellations. Concepts and Applications of the Voronoi Diagrams*; John Wiley and Sons: New York, 1992.
(32) Luchnikov, V. A.; Medvedev, N. N.; Oger, L.; Troadec, J. P. *Phys. Rev. E* **1999**, *59*, 7205.
(33) Medvedev, N. N. In *Voronoi's impact on modern science*; Engel, P., Syta, H., Eds.; Institute of Mathematics: Kiev, 1998; p 164.
(34) Medvedev, N. N. *The Voronoi-Delaunay method in the structural investigation of noncrystalline systems*; SB RAS: Novosibirsk, 2000, in Russian.
(35) Aurenhammer, F. *ACM Comput. Surv.* **1991**, *23*, 345.
(36) Gavrilova, M. Proximity and Applications in General Metrics. Ph.D. Thesis: University of Calgary, 1998.
(37) Kim, D. S.; Kim, D.; Sugihara, K. *Comput. Aided Geom. Design* **2001**, *18*, 541.
(38) Kim, D. S.; Kim, D.; Sugihara, K. *Comput. Aided Geom. Design* **2001**, *18*, 563.
(39) Karavelas M. I.; Yvinec, M. *Technical Report No. 4466*; INRIA Sophia Antipolis; URL http://www-sop.inria.fr/prisme/biblio/Keyword/VORONOI-DIAGRAMS.html.
(40) Will, H. M. *Technical Report #300, #302*; ETH Zuerich; URL ftp://ftp.inf.ethz.ch/pub/publications/tech-reports.
(41) Richard, P.; Oger, L.; Troadec, J. P.; Gervois, A. *Eur. Phys. J. E* **2001**, *6*, 295.
(42) Goede, A.; Preissner, R.; Froemmel, C. *J. Comput. Chem.* **1997**, *18*, 1113.
(43) Medvedev N. N.; Voloshin, V. P. Manuscript in preparation.
(44) Singh, R. K.; Tropsha, A.; Vaisman, I. I. *J. Comput. Biol.* **1996**, *3*, 213.
(45) Marrink S. J.; Berendsen, H. J. C. *J. Phys. Chem.* **1994**, *98*, 4155.
(46) Marrink S. J.; Berendsen, H. J. C. *J. Phys. Chem.* **1996**, *100*, 16729.
(47) Jedlovszky P.; Mezei, M. *J. Am. Chem. Soc.* **2000**, *122*, 5125.

(48) Jedlovszky P.; Mezei, M. *J. Phys. Chem. B* **2003**, *107*, 5322.
(49) Marrink, S. J.; Sok, R. M.; Berendsen, H. J. C. *J. Chem. Phys.* **1996**, *104*, 9090.
(50) Naberukhin, Y. I.; Voloshin, V. P.; Medvedev, N. N. *Mol. Phys.* **1991**, *73*, 917.
(51) Voloshin, V. P.; Naberukhin, Y. I.; Medvedev, N. N. *Zh. Phys. Khim.* **1992**, *66*, 155 (in Russian).
(52) Sastry, S.; Corti, D. S.; Debenedetti, P. G.; Stillinger, F. H. *Phys. Rev. E* **1997**, *56*, 5524.
(53) Venable, R. M.; Zhang, Y.; Hardy, B. J.; Pastor, R. W. *Science* **1993**, *262*, 223.
(54) Chiu, S. W.; Clark, M.; Balaji, V.; Subramaniam, S.; Scott, H. L.; Jakobson, E. *Biophys. J.* **1995**, *69*, 1230.
(55) Tu, K.; Tobias, D. J.; Klein, M. L. *Biophys. J.* **1995**, *69*, 2558.
(56) Perera, L.; Essmann, U.; Berkowitz, M. L. *Langmuir* **1996**, *12*, 2625.
(57) Jedlovszky P.; Mezei, M. *J. Chem. Phys.* **1999**, *111*, 10770.
(58) Zubrzycki, I. Z. Xu, Y. Madrid, M. and Tang, P. *J. Chem. Phys.* **2000**, *112*, 3437.
(59) Jedlovszky P.; Mezei, M. *J. Phys. Chem. B* **2001**, *105*, 3614.
(60) Rabinovich, A. L.; Ripatti, P. O.; Balabaev, N. K.; Leermakers, F. A. M. *Phys. Rev. E* **2003**, *67*, 011909.
(61) Jedlovszky P.; Mezei, M. *J. Phys. Chem. B* **2003**, *107*, 5311.
(62) Jedlovszky P.; Medvedev, N. N.; Mezei, M. *J. Phys. Chem. B* **2004**, *108*, 465.
(63) Schlenkirch, M.; Brickmann, J.; MacKerrel, A. D., Jr.; Karplus, M. In *Biological Membranes*; Merz, K. M., Roux, B., Eds.; Birkhäuser: Boston, 1996; pp 31−82.
(64) Jorgensen, W. L.; Chandrashekar, J.; Madura, J. D.; Impey, R.; Klein, M. L. *J. Chem. Phys.* **1983**, *79*, 926.
(65) Anikeenko, A. V.; Alinchenko, M. G.; Voloshin, V. P.; Medvedev, N. N.; Gavrilova, M. L.; Jedlovszky, P. In *Proceedings of the 4th Workshop of Computational Geometry and Applications, Lecture Notes in Computer Science 3045*; Springer-Verlag: Berlin, 2004; Vol. III, pp 217−226.
(66) Rashin, A. A. *J. Phys. Chem. B* **1989**, *93*, 4664.
(67) Resat, H.; Marrone, T. J.; McCammon, J. A. *Biophys. J.* **1997**, *72*, 522.